Supplement

Maintenance DNA methylation is essential for regulatory T cell development and stability of suppressive function

Kathryn A. Helmin,[1] Luisa Morales-Nebreda,[1] Manuel A. Torres Acosta,[1] Kishore R. Anekalla,[1] Shang-Yang Chen,[1] Hiam Abdala-Valencia,[1] Yuliya Politanska,[1] Paul Cheresh,[1] Mahzad Akbarpour,[2] Elizabeth M. Steinert,[1] Samuel E. Weinberg,[1,3] and Benjamin D. Singer[1,4,5,*]

[1]Division of Pulmonary and Critical Care Medicine, Department of Medicine
Northwestern University Feinberg School of Medicine
Chicago, IL 60611 USA

[2]Department of Surgery
Northwestern University Feinberg School of Medicine
Chicago, IL 60611 USA

[3]Department of Pathology
Northwestern University Feinberg School of Medicine
Chicago, IL 60611 USA

[4]Department of Biochemistry and Molecular Genetics
Northwestern University Feinberg School of Medicine
Chicago, IL 60611 USA

[5]Simpson Querrey Institute for Epigenetics
Northwestern University Feinberg School of Medicine
Chicago, IL 60611 USA

*To whom correspondence should be addressed:
Benjamin D. Singer, MD
Division of Pulmonary and Critical Care Medicine, Department of Medicine
Department of Biochemistry and Molecular Genetics
Simpson Querrey Institute for Epigenetics
Northwestern University Feinberg School of Medicine
303 E. Superior St.
Simpson Querrey, 5th Floor
Chicago, IL 60611 USA
benjamin-singer@northwestern.edu
Tel: (312) 503-4494
Fax: (312) 503-0411

Supplemental Figures

Supplemental Figure 1

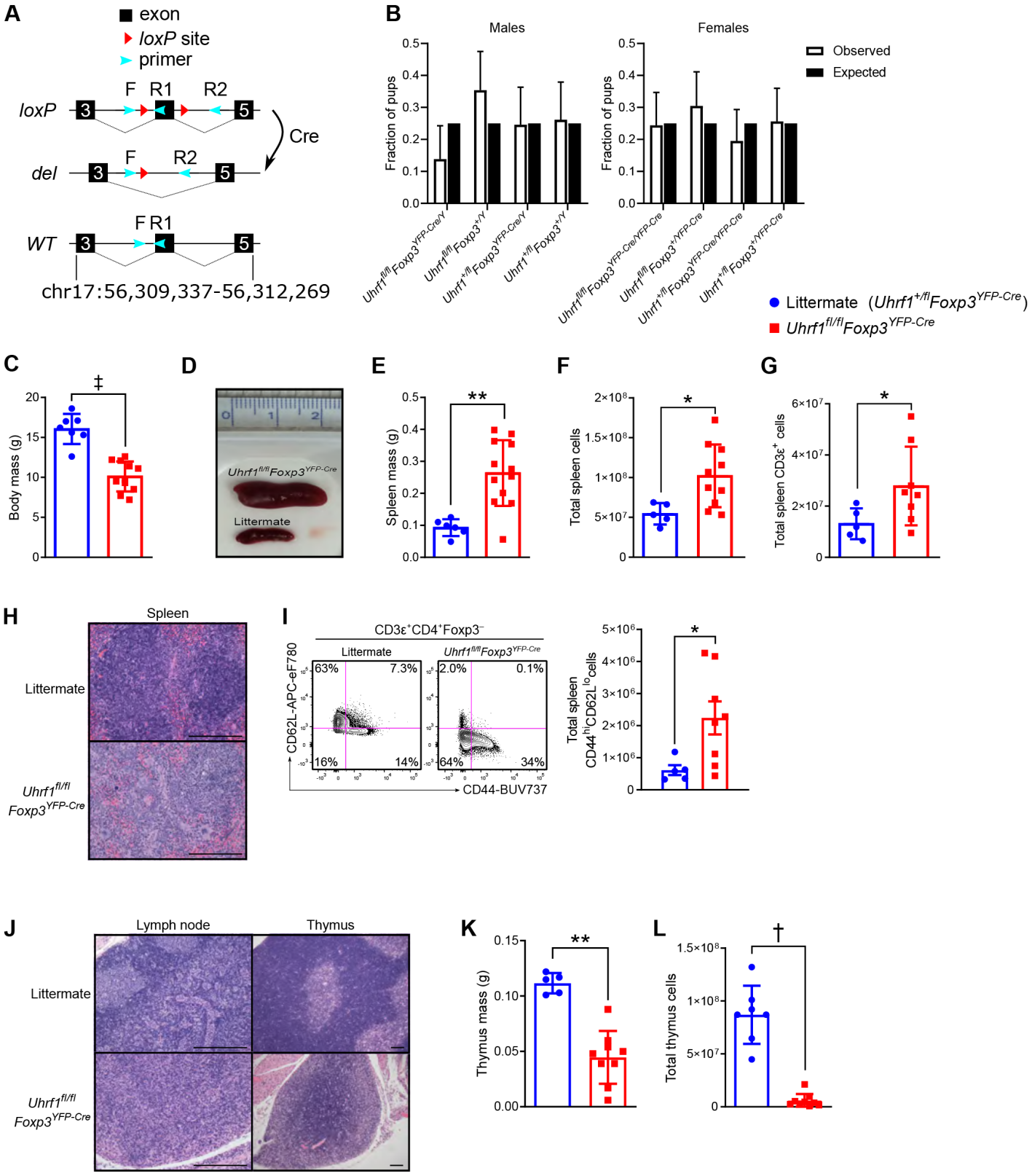

Supplemental Figure 1. Inflammatory phenotype of 3-4-week-old Treg cell-specific Uhrf1-deficient mice. (**A**) Schematic of the *Uhrf1* locus demonstrating the positions of exons, *loxP* sites, and primers used for genotyping. (**B**) Observed and expected frequencies of F1 pups resulting from crosses of male *Uhrf1*$^{+/fl}$*Foxp3*$^{YFP\text{-}Cre/Y}$ mice with female *Uhrf1*$^{fl/fl}$*Foxp3*$^{+/YFP\text{-}Cre}$ mice. Chi-square test for goodness of fit $p = 0.11$ for male offspring and 0.57 for female offspring. Chi-square = 6.1 for males and 2.0 for females, both with 3 degrees of freedom. $n = 65$

males and 82 females. (**C**) Body mass of littermate control (*Uhrf1*$^{+/fl}$*Foxp3*$^{YFP\text{-}Cre}$, *n* = 7) and *Uhrf1*$^{fl/fl}$*Foxp3*$^{YFP\text{-}Cre}$ (*n* = 11) mice. (**D**) Gross spleen photomicrographs with cm-ruler. (**E**) Splenic masses from littermate (*n* = 6) and *Uhrf1*$^{fl/fl}$*Foxp3*$^{YFP\text{-}Cre}$ (*n* = 12) mice. (**F**) Spleen cellularity of littermate (*n* = 5) and *Uhrf1*$^{fl/fl}$*Foxp3*$^{YFP\text{-}Cre}$ (*n* = 10) mice. (**G**) Spleen CD3ε^{+} T cell numbers from littermate (*n* = 5) and *Uhrf1*$^{fl/fl}$*Foxp3*$^{YFP\text{-}Cre}$ (*n* = 8) mice. (**H**) Photomicrographs of spleen. Scale bar represents 100 μm. (**I**) Activation state of splenic CD3ε^{+}CD4^{+}Foxp3^{-} cells. Representative contour plots and summary data of CD44^{hi}CD62L^{lo} cells are shown. *n* = 5 (littermate) and 8 (*Uhrf1*$^{fl/fl}$*Foxp3*$^{YFP\text{-}Cre}$). (**J**) Photomicrographs of lymph node and thymus. Scale bar represents 100 μm. (**K**) Thymic mass of littermate (*n* = 5) and *Uhrf1*$^{fl/fl}$*Foxp3*$^{YFP\text{-}Cre}$ (*n* = 9) mice. (**L**) Thymus cellularity of littermate (*n* = 7) and *Uhrf1*$^{fl/fl}$*Foxp3*$^{YFP\text{-}Cre}$ (*n* = 9) mice. Summary plots show all data points with mean and standard deviation except for (B), which shows mean and 95% confidence interval (Wilson/Brown method). * $p < 0.05$, ** $p < 0.01$, † $p < 0.001$, ‡ $p < 0.0001$ by Mann-Whitney test; exact *p*-values are in Source Data. See Supplemental Table 3 for fluorochrome abbreviations.

Supplemental Figure 2

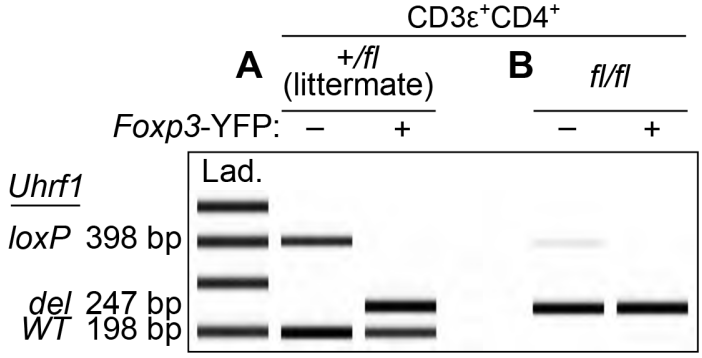

Supplemental Figure 2. Genotype of sorted splenic CD3ε^{+}CD4^{+} T cell populations. (**A and B**) Agilent TapeStation image of PCR products generated using the displayed primer scheme shown in Supplemental Figure 1A. Splenic CD3ε^{+}CD4^{+} cells were sorted based on *Foxp3*-YFP status from 3-4-week-old *Uhrf1*$^{+/fl}$*Foxp3*$^{YFP\text{-}Cre}$ littermate control mice (A) and *Uhrf1*$^{fl/fl}$*Foxp3*$^{YFP\text{-}Cre}$ mice (B). Image is representative of three independent experiments. Lad., ladder.

Supplemental Figure 3

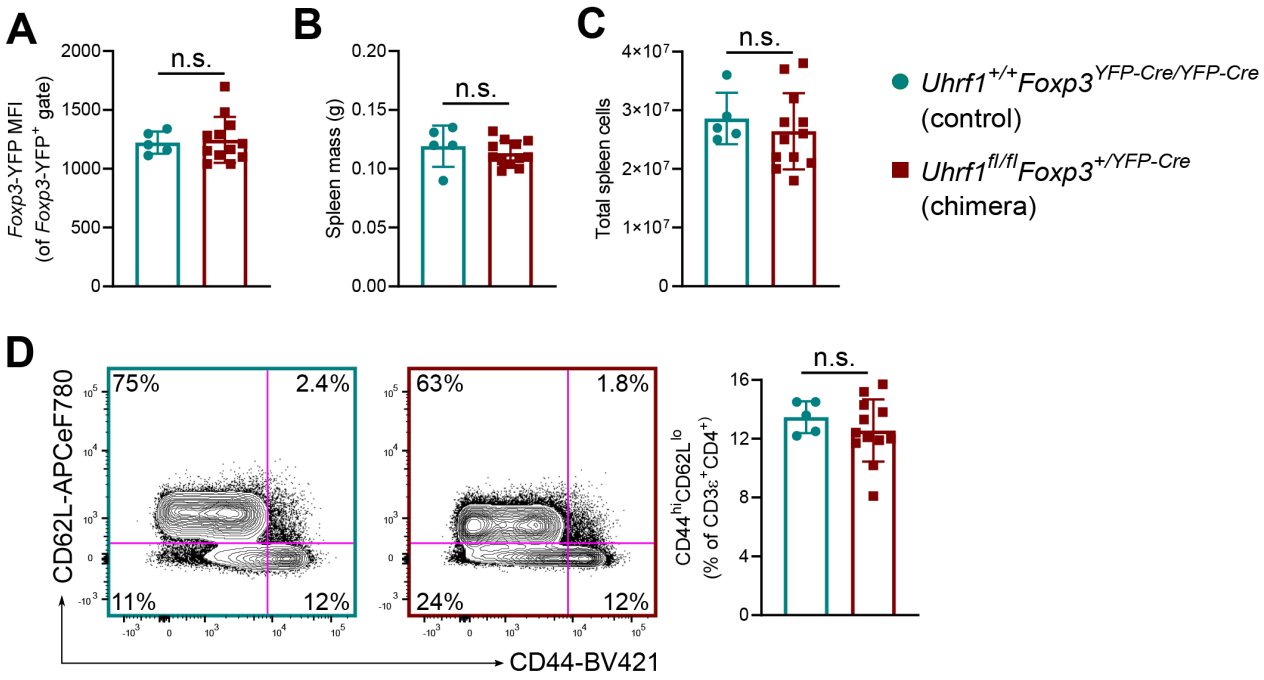

Supplemental Figure 3. Extended phenotype of Treg cell-specific Uhrf1 chimeric knockout mice. (**A**) *Foxp3*-YFP mean fluorescence intensity (MFI) within the splenic *Foxp3*-YFP$^+$ population of 8-week-old female *Uhrf1*$^{+/+}$*Foxp3*$^{YFP\text{-}Cre/YFP\text{-}Cre}$ (control) and *Uhrf1*$^{fl/fl}$*Foxp3*$^{+/YFP\text{-}Cre}$ (chimeric) mice. (**B**) Splenic mass of control and chimeric mice. (**C**) Spleen cellularity of control and chimeric mice. (**D**) Activation state of splenic CD3ε$^+$CD4$^+$ cells. Representative contour plots and summary data of CD44^{hi}CD62L^{lo} cells are shown. Summary plots show all data points with mean and standard deviation. *n* = 5 (control) and 12 (chimera). n.s. not significant by Mann-Whitney test; exact *p*-values are in Source Data. See Supplemental Table 3 for fluorochrome abbreviations.

Supplemental Figure 4

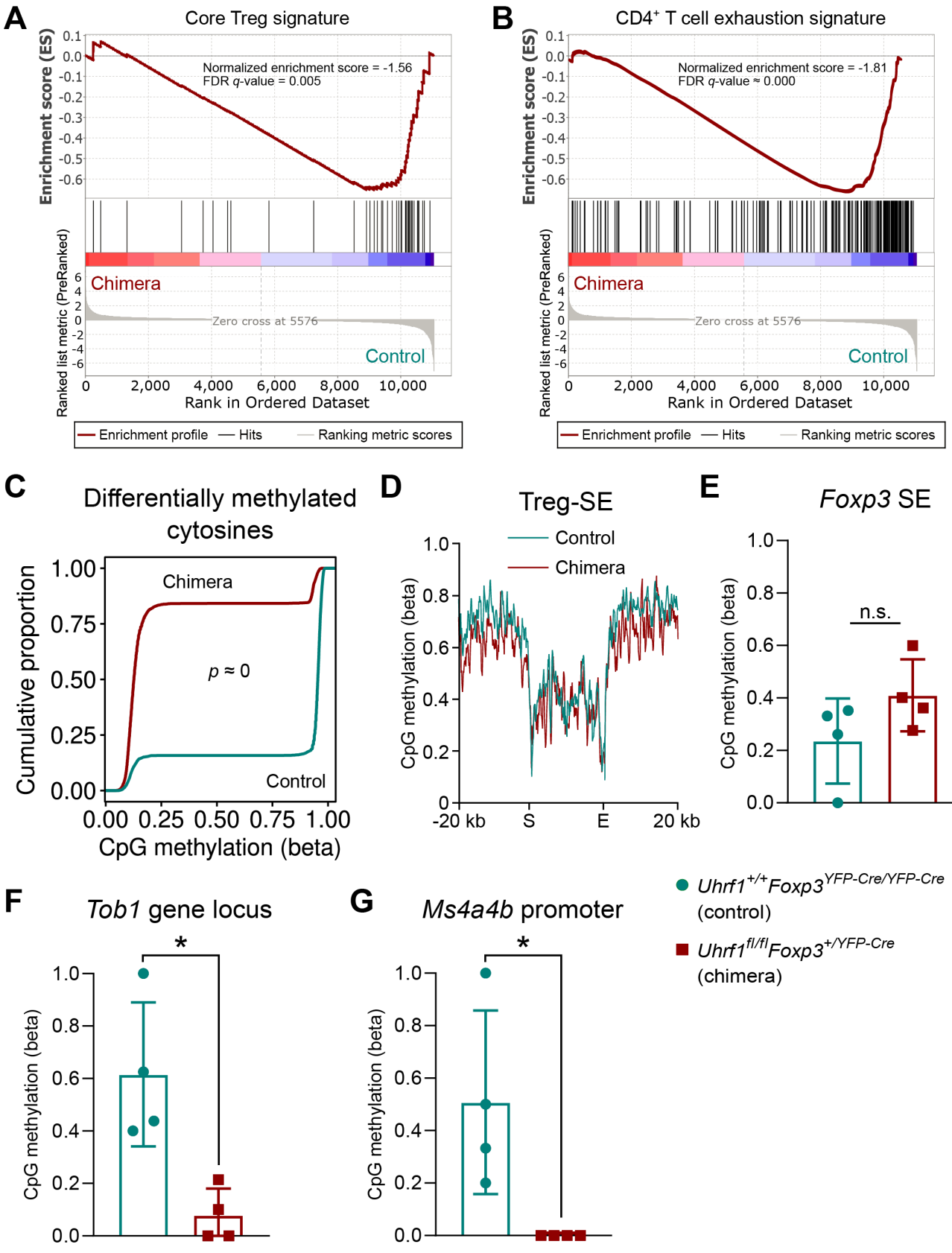

Supplemental Figure 4. Extended molecular analysis of Treg cell-specific Uhrf1 chimeric knockout mice. (**A and B**) Gene set enrichment plots testing for enrichment of a Treg cell-defining gene set (1) (A) and a CD4$^+$ T cell exhaustion gene set (2) (B) with genes ordered by log2(fold-change) in average expression comparing

CD3ε^{+}CD4^{+}CD25^{hi}*Foxp3*-YFP^{+} cells from Uhrf1 chimeric knockout mice against control mice. The normalized enrichment scores (NES) and FDR *q*-values associated with these tests are shown. (**C**) Cumulative distribution function plot of 4,708 CpGs with FDR *q*-value < 0.05 compared using a Wald test for beta-binomial distributions. (**D**) Metagene analysis of CpG methylation across the start (S) through the end (E) of Treg cell-specific super-enhancer elements (Treg-SE) as defined in reference (3). (**E-G**) CpG methylation status of the *Foxp3* locus super-enhancer (D, chrX:7,565,077-7,587,439), the *Tob1* gene locus (E, chr11:94,209,454-94,217,495), and the *Ms4a4b* promoter (F, chr19:11,442,553-11,444,553). *n* = 4 mice per group. Summary plots show all data points with mean and standard deviation. The asymptotic *p*-value resulting from a Kolmogorov-Smirnov test for cumulative distributions is shown in (C). * $p < 0.05$, n.s. not significant by Mann-Whitney test (E-G); exact *p*-values are in Source Data.

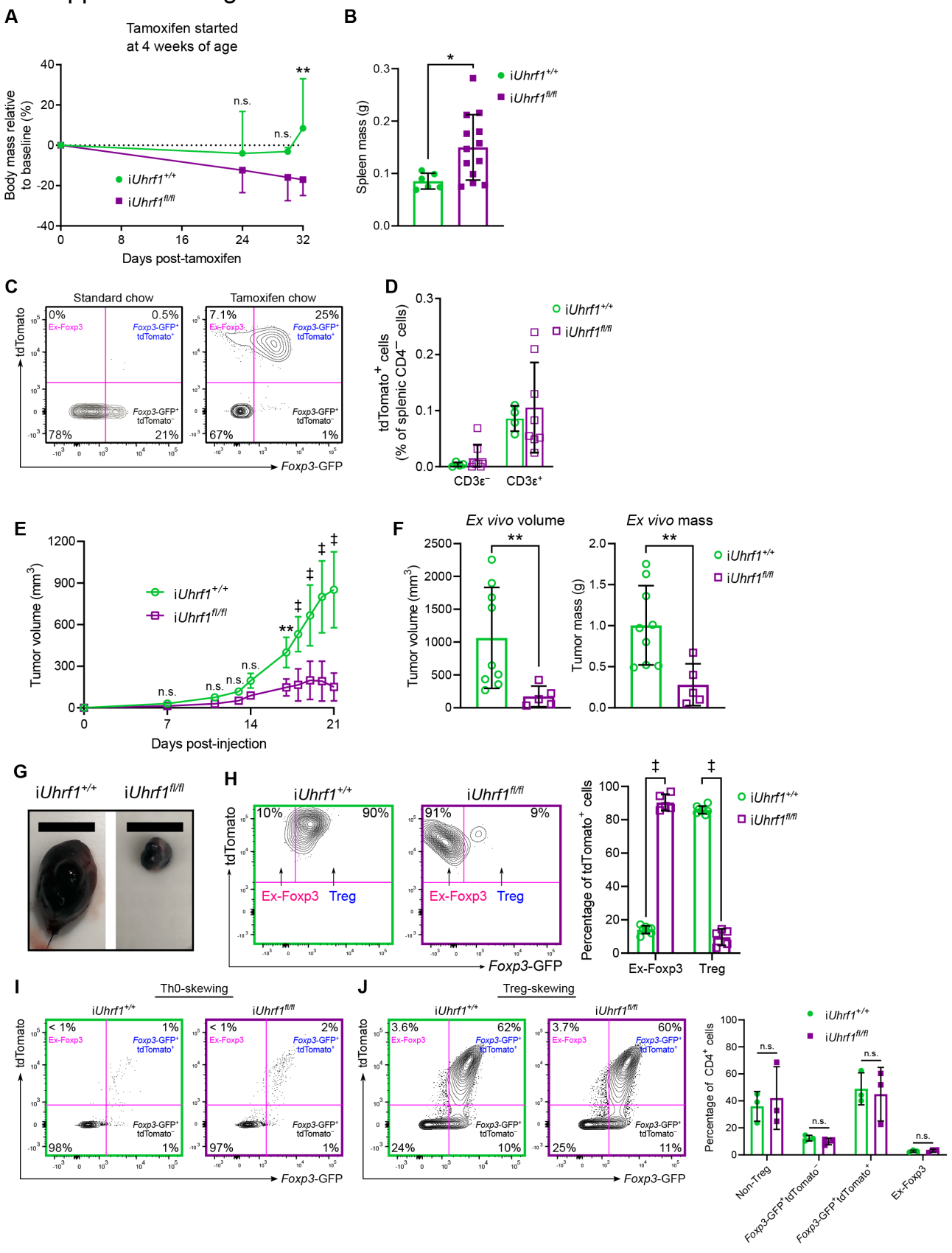

Supplemental Figure 5. Phenotype of i*Uhrf1*$^{fl/fl}$ mice after initiation of tamoxifen at 4 weeks of age, validation of the Foxp3^{+} lineage-tracing construct, and results of the B16 melanoma and iTreg cell generation experiments. (**A**) Body mass curves for i*Uhrf1*$^{+/+}$ (n = 6) and i*Uhrf1*$^{fl/fl}$ (n = 21) mice initiated on tamoxifen at 4 weeks of age.

(**B**) Spleen masses for i*Uhrf1*$^{+/+}$ (n = 6) and i*Uhrf1*$^{fl/fl}$ (n = 13) mice after 4 weeks of tamoxifen. (**C**) 8-week-old i*Uhrf1*$^{+/+}$ mice received either standard chow or tamoxifen chow for 4 weeks. Representative contour plots of splenic CD3ε^{+}CD4^{+} cells are shown. (**D**) 8-week-old i*Uhrf1*$^{+/+}$ (n = 4) and i*Uhrf1*$^{fl/fl}$ (n = 8) mice received tamoxifen chow for 4 weeks. (**E**) Growth of B16 melanoma cells in i*Uhrf1*$^{+/+}$ and i*Uhrf1*$^{fl/fl}$ mice. Tamoxifen chow was administered to 8-week-old mice beginning 3 weeks before tumor cell injection. (**F**) Ex vivo tumor volumes and masses measured after post-mortem tumor resection on day 21 post-injection. (**G**) Photomicrographs of resected tumors. Scale bar represents 1 cm. Tumor experiments were performed over two separate experiments with total n = 9 (i*Uhrf1*$^{+/+}$) and 5 (i*Uhrf1*$^{fl/fl}$). (**H**) Representative flow cytometry contour plots gated on splenic CD3ε^{+}CD4^{+}tdTomato^{+} cells showing the percentage of intra-tumoral ex-Foxp3 (*Foxp3*-GFP^{-}) and Treg (*Foxp3*-GFP^{+}) cells, summarized in the accompanying graph. n = 8 (i*Uhrf1*$^{+/+}$) and 5 (i*Uhrf1*$^{fl/fl}$). (**I and J**) Naïve CD4^{+} T cells from i*Uhrf1*$^{+/+}$ and i*Uhrf1*$^{fl/fl}$ mice were cultured under Th0 (I) or Treg (J) cell-skewing conditions for 3 days in the presence of tamoxifen (n = 3 mice per group). Representative contour plots of live CD4^{+} cells are shown with accompanying summary data for the Treg cell-skewing condition. Summary plots show all data points with mean and standard deviation. * $p < 0.05$, ** $p < 0.01$, ‡ p or $q < 0.0001$, n.s. not significant by two-way ANOVA with Sidak's *post-hoc* testing for multiple comparisons (A and E), Mann-Whitney test (B and F), or the two-stage linear step-up procedure of Benjamini, Krieger, and Yekutieli with Q = 5% (H and J); exact p- and q-values are in Source Data. For the comparison between genotypes in (A), F(DFn, DFd) = F(1, 59) = 14.6 with $p = 0.0003$. For the comparison between genotypes in (E), F(DFn, DFd) = F(1, 120) = 130.0 with $p < 0.0001$.

Supplemental Figure 6

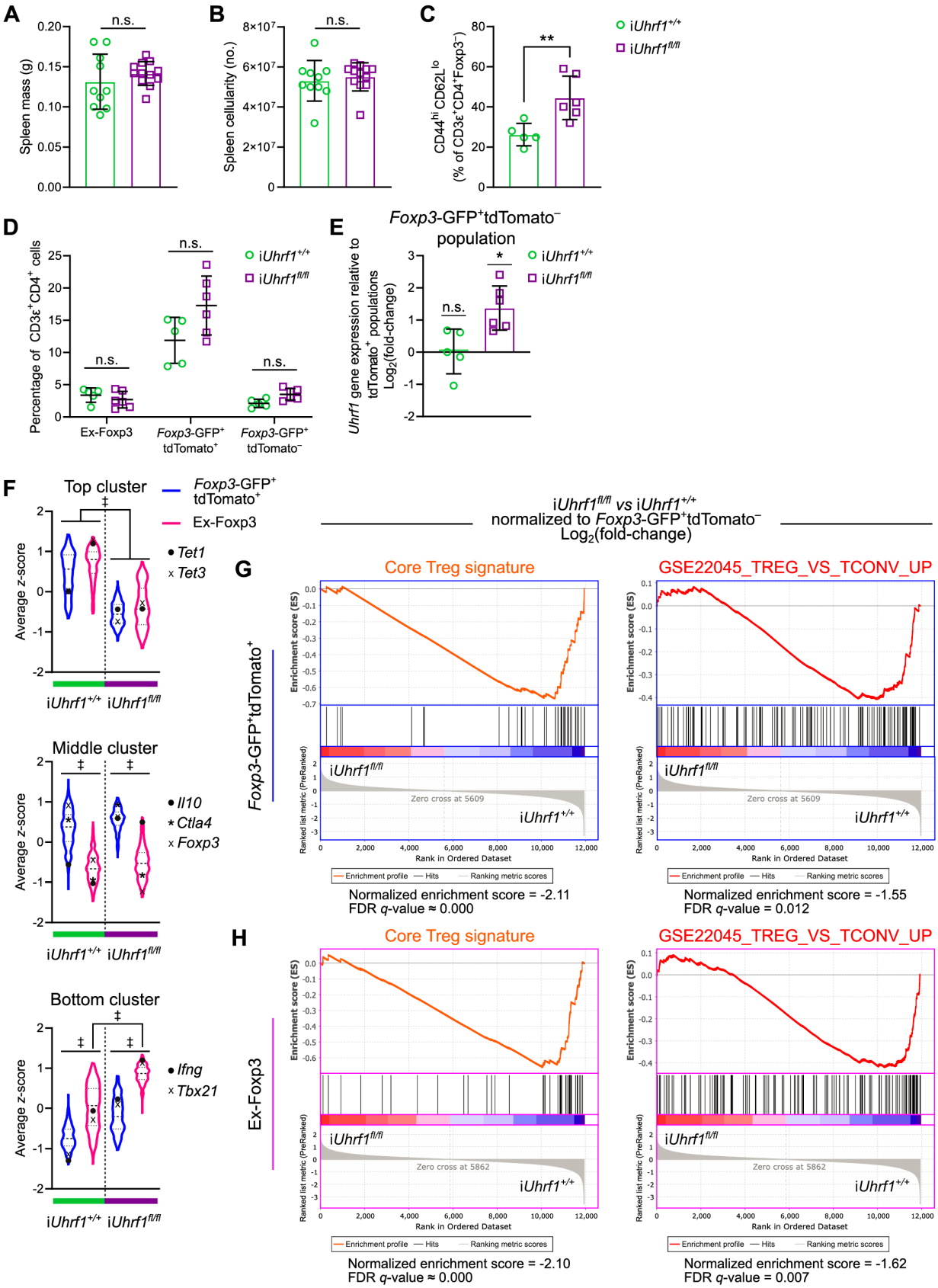

Supplemental Figure 6. Extended phenotypic and transcriptional analysis of the pulse-chase model. (**A**) Splenic mass of i*Uhrf1*$^{+/+}$ (n = 10) and i*Uhrf1*$^{fl/fl}$ (n = 12) mice after a 2-week pulse of tamoxifen chow followed by 4 weeks of standard chow. (**B**) Spleen cellularity of i*Uhrf1*$^{+/+}$ (n = 10) and i*Uhrf1*$^{fl/fl}$ (n = 12) mice. (**C**) Activation state of

splenic CD3ε$^+$CD4$^+$Foxp3$^-$ cells. *n* = 5 (i*Uhrf1*$^{+/+}$) and 6 (i*Uhrf1*$^{fl/fl}$). (**D**) Summary data of splenic live CD3ε$^+$CD4$^+$ cell subsets. *n* = 5 (i*Uhrf1*$^{+/+}$) and 6 (i*Uhrf1*$^{fl/fl}$). (**E**) *Uhrf1* gene expression in *Foxp3*-GFP$^+$tdTomato$^-$ cells relative to the tdTomato$^+$ populations. *n* = 5 (i*Uhrf1*$^{+/+}$) and 6 (i*Uhrf1*$^{fl/fl}$). (**F**) Average *z*-scores for the top, middle, and bottom *k*-means clusters shown in Figure 6D. The positions of selected genes within the distributions are shown. (**G and H**) Gene set enrichment plots testing for enrichment of a Treg cell-defining gene set (1) or the GSE22045_TREG_VS_TCONV_UP gene set (4) with genes ordered by log2(fold-change) in average expression comparing *Foxp3*-GFP$^+$tdTomato$^+$ (G) or ex-Foxp3 (H) cells from i*Uhrf1*$^{fl/fl}$ versus i*Uhrf1*$^{+/+}$ mice. Expression values are normalized to the *Foxp3*-GFP$^+$tdTomato$^-$ population sorted from the respective genotype. The normalized enrichment scores (NES) and FDR *q*-values associated with these tests are shown. Summary plots show all data points with mean and standard deviation; violin plots show median and quartiles. *n* = 5 (i*Uhrf1*$^{+/+}$) and 6 (i*Uhrf1*$^{fl/fl}$). * $p < 0.05$, ** $p < 0.01$, ‡ $q < 0.0001$, n.s. not significant by Mann-Whitney test (A-C), the two-stage linear step-up procedure of Benjamini, Krieger, and Yekutieli with *Q* = 5% (D), one-way ANOVA (E), or a mixed-effects analysis with the two-stage linear step-up procedure of Benjamini, Krieger, and Yekutieli with *Q* = 5% (F); exact *p*- and *q*- values are in Source Data. For the comparisons in (E) between i*Uhrf1*$^{+/+}$ cell populations, F(DFn, DFd) = F(2, 12) = 1.4 with $p = 0.28$; for i*Uhrf1*$^{fl/fl}$ cell populations, F(DFn, DFd) = F(2, 15) = 4.3 with $p = 0.03$.

Supplemental Figure 7

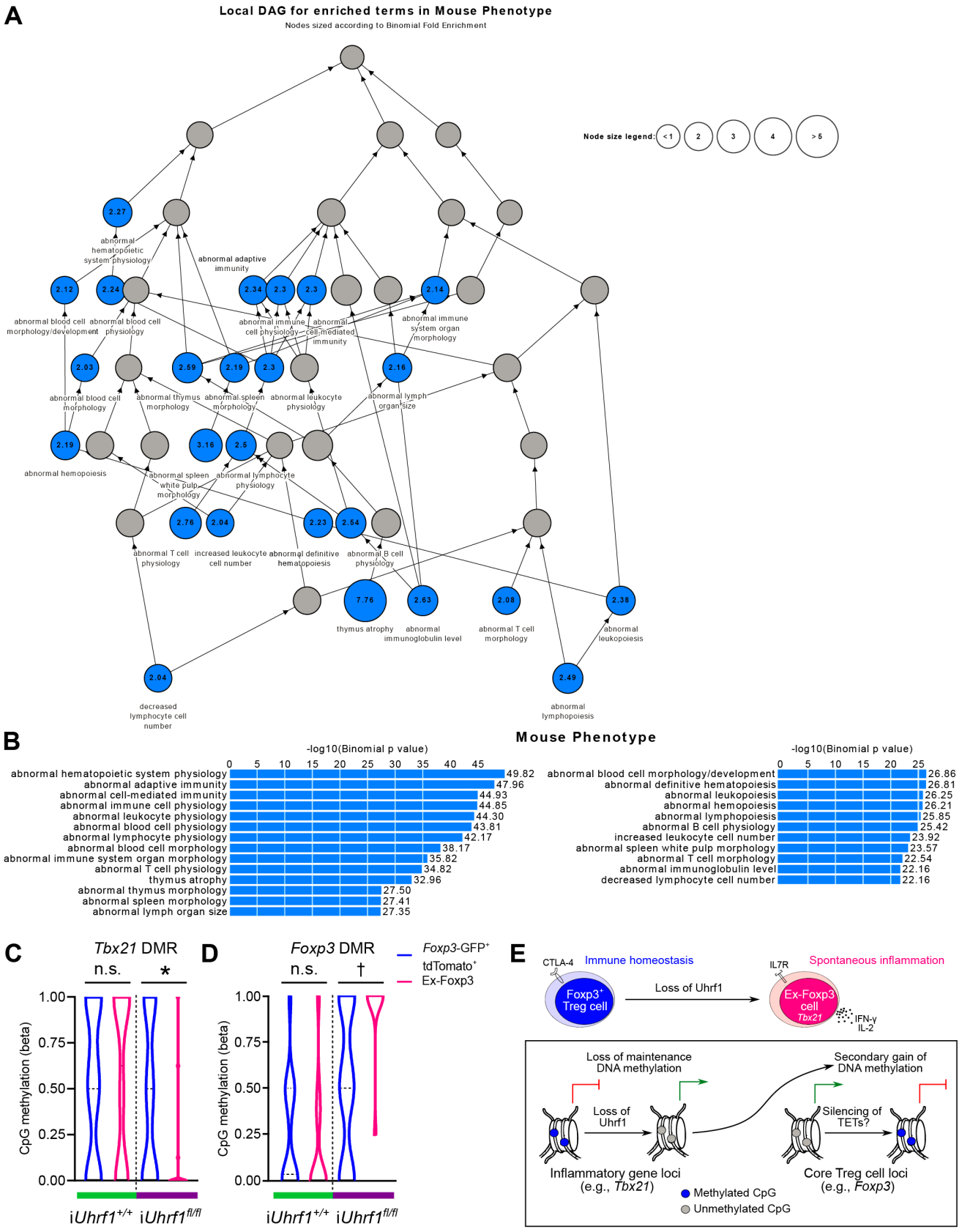

Supplemental Figure 7. Extended DNA methylation analysis of the pulse-chase model. (**A**) Directed acyclic graph (DAG) based on the enriched terms (shown in blue) from the Mouse Genome Informatics Phenotype ontology (5). Nodes are sized according to binomial fold enrichment. (**B**) Bar chart of binomial *p*-values based

on the analysis shown in (A). (**C and D**) CpG methylation at the differentially methylated region (DMR) located at the *Tbx21* locus (C, chr11:97,112,193-97,113,285) and the *Foxp3* locus (D, chrX:7,580,236-7,581,944). (**E**) Graphical abstract of the proposed model. Violin plots show median and quartiles. n = 4 mice per cell type for both genotypes. * $q < 0.05$, † $q < 0.001$, n.s. not significant by a mixed-effects analysis with the two-stage linear step-up procedure of Benjamini, Krieger, and Yekutieli with Q = 5% (C and D); exact q-values are in Source Data.

Supplemental Tables

Supplemental Table 1. Gene Set Enrichment Analysis report of positively-enriched gene sets: *Foxp3*-GFP^{+}tdTomato^{+} cells. The ranked gene list used to generate Figure 6G (*Foxp3*-GFP^{+}tdTomato^{+} cells of i*Uhrf1*$^{fl/fl}$ versus i*Uhrf1*$^{+/+}$ normalized to their respective *Foxp3*-GFP^{+}tdTomato^{-} population) against a comprehensive list of 4,872 Immunologic Signature gene sets housed in the Molecular Signatures Database. [provided as a tab-delimited file]

Supplemental Table 2. Gene Set Enrichment Analysis report of positively-enriched gene sets: ex-Foxp3 cells. The ranked gene list used to generate Figure 6H (ex-Foxp3 cells of i*Uhrf1*$^{fl/fl}$ versus i*Uhrf1*$^{+/+}$ normalized to their respective *Foxp3*-GFP^{+}tdTomato^{-} population) against a comprehensive list of 4,872 Immunologic Signature gene sets housed in the Molecular Signatures Database. [provided as a tab-delimited file]

Supplemental Table 3. Reagents and cytometer setup. FITC, fluorescein isothiocyanate; PerCP, peridinin chlorophyll protein complex; PE, phycoerythrin; APC, allophycocyanin; BV, Brilliant Violet; BUV, Brilliant UltraViolet.

Antigen/ reagent	Conjugate	Clone	Company	Catalog number	Volume (µL) added to stain cells in 100 µL	Laser line (color)	Bandpass filter	Longpass filter
CD3ε	FITC	145-2C11	eBioscience	11-0031	0.75	488 nm (blue)	530/30	505LP
CD4	PerCP-Cy5.5	GK1.5	BioLegend	100434	1	488 nm (blue)	710/50	685LP
Ki-67	PerCP-eFluor710	SolA15	eBioscience	46-5698-82	0.75	488 nm (blue)	710/50	685LP
CD3ε	PE	145-2C11	eBioscience	12-0031-83	0.25	561 nm (yellow-green)	586/15	-
CD25	PE	PC61.5	eBioscience	12-0251-82	0.5	561 nm (yellow-green)	586/15	-
IL-17A	PE	TC11-18H10	BD Biosciences	561020	1	561 nm (yellow-green)	586/15	-
CD8	PE-CF594	53-6.7	BioLegend	100762	0.25	561 nm (yellow-green)	610/20	595LP
IFN-γ	PE-CF594	XMG1.2	BD Biosciences	562333	1	561 nm	610/20	595LP

						(yellow-green)		
Foxp3	PE-Cy7	FJK-16s	eBioscience	25-5773-82	1	561 nm (yellow-green)	780/60	750LP
CD25	APC	PC61.5	eBioscience	17-0251-82	0.5	637 nm (red)	670/30	-
IL-4	APC	11B11	BD Biosciences	562045	1	637 nm (red)	670/30	-
CD62L	APC-eFluor780	MEL-14	eBioscience	47-0621-82	0.25	637 nm (red)	780/60	750LP
CD4	APC-eFlour780	RM4-5	eBioscience	47-0042-82	0.5	637 nm (red)	780/60	750LP
CD3ε	BV421	145-2C11	BioLegend	100341	0.75	405 nm (violet)	450/50	-
CTLA4	BV421	UC10-4B9	BioLegend	106312	1	405 nm (violet)	450/50	-
Annexin V	Pacific Blue	-	Invitrogen	A35122	5	405 nm (violet)	450/50	-
Live-dead marker	eFluor506	-	eBioscience	65-0866-14	Per manufacturer's protocol	405 nm (violet)	525/50	505LP
Live-dead marker	LIVE/DEAD Fixable Blue Stain	-	Molecular Probes	L23105	Per manufacturer's protocol	355 nm (UV)	450/50	410LP

CD4	BUV395	GK1.5	BD Biosciences	563790	0.5	355 nm (UV)	379/28	-
CD44	BUV737	IM7	BD Biosciences	564392	0.5	355 nm (UV)	750/50	635LP

References Included in the Supplement

1. Hill JA, et al. Foxp3 transcription-factor-dependent and -independent regulation of the regulatory T cell transcriptional signature. *Immunity.* 2007;27(5):786-800.

2. Crawford A, et al. Molecular and transcriptional basis of CD4(+) T cell dysfunction during chronic infection. *Immunity.* 2014;40(2):289-302.

3. Kitagawa Y, et al. Guidance of regulatory T cell development by Satb1-dependent super-enhancer establishment. *Nat Immunol.* 2017;18(2):173-183.

4. Bonacci B, et al. Requirements for growth and IL-10 expression of highly purified human T regulatory cells. *J Clin Immunol.* 2012;32(5):1118-1128.

5. Blake JA, Bult CJ, Eppig JT, Kadin JA, Richardson JE, Mouse Genome Database G. The mouse genome database genotypes::Phenotypes. *Nucleic Acids Res.* 2009;37(Database issue):D712-719.